Journal of Magnetism and Magnetic Materials 340 (2013) 1–4

Contents lists available at SciVerse ScienceDirect

Journal of Magnetism and Magnetic Materials

journal homepage: www.elsevier.com/locate/jmmm

Exchange bias effect in $Tb_{0.4}Dy_{0.6}MnO_3$

M.H. Xu [a,*], Z.H. Wang [b], D.W. Zhang [b], Y.W. Du [b]

[a] Department of Applied Physics, Nanjing University of Technology, Nanjing 210009, China
[b] National Laboratory of Solid State Microstructure, Department of Physics, Nanjing University, Nanjing 210093, China

ARTICLE INFO

Article history:
Received 1 September 2012
Received in revised form
7 March 2013
Available online 26 March 2013

Keywords:
Manganite
Exchange bias
Antiferromagnet
Ferromagnet

ABSTRACT

Polycrystalline $Tb_{1-x}Dy_xMnO_3$ ($x=0.0$, 0.3, 0.5, 0.6, and 0.8) were prepared by the traditional solid-phase reaction method. The XRD result shows that $Tb_{0.4}Dy_{0.6}MnO_3$ may have a different structure; it has two diffraction peaks near 33.30° while other samples have three diffraction peaks at the same diffraction angle. The magnetic properties of $Tb_{0.4}Dy_{0.6}MnO_3$ are also different from those of the other samples. An exchange-bias effect was observed at 5 K with the field cooling of ± 5 T for $Tb_{0.4}Dy_{0.6}MnO_3$. The dc and ac magnetizations as well as magnetic hysteresis measurements suggest the coexistence of antiferromagnet and ferromagnet characteristics which originate from the interplay of 3d and 4f electrons at the rare-earth sublattice and low temperature in $Tb_{0.4}Dy_{0.6}MnO_3$.

1. Introduction

In recent years perovskite-type manganites ($RMnO_3$, R stands for "rare-earth" ions) have attracted considerable interest due to the appearance of complex magnetic property and magnetoelectric coupling [1,2] as well as the potential applications in spintronics, magnetic sensing and recording devices [3–8]. A lot of works in manganites have proved to be technologically promising, which include exchange bias (EB) [9–12], multiferroicity [13–15], and memory effect [16,17]. A major part of the investigations focused on hole doping such as doping of divalent alkali atoms or isovalent doping at the R site. Doping of divalent alkali atoms in $RMnO_3$ leads to a mixed-valent state of Mn which plays a crucial role in determining the structural and electromagnetic properties of the compounds. Compared with doping of divalent alkali atoms, isovalent doping at the R site creates only Mn^{3+} which can lead to dominating Jahn–Teller (JT) distortion. Moreover it can be probed through isovalent doping that the effect of ionic size mismatch leads to strain in the crystal structure. Recently there are lots of investigations on the effect of ionic size mismatch, such as $Eu_{1-x}Y_xMnO_3$ [18,19], $La_{1-x}Eu_xMnO_3$ [20], and $La_{1-x}Gd_xMnO_3$ [21]. Furthermore, the great mass of research has concentrated on a significant difference in ionic radius of doping element at the R site. To the best of our knowledge, compared to significant difference radius doping, studies on the tiny difference radius doping at the R site are few. From a general point of view, the rare-earth manganites can be grouped into two classes: the compounds from La to Dy (with the exception of Ce and Pm), characterized by larger ionic radii, reveal an orthorhombic perovskite-derived structure; while the compounds from Ho to Lu crystallize in a hexagonal structure, are not related to the perovskites [22]. Dy^{3+} ionic radius (0.091 nm) approximates that of Tb^{3+} (0.092 nm). Herein, we focused on the tiny difference radius isovalent substituted at the R site in manganite $TbMnO_3$ and reported the structural and magnetic properties of $Tb_{1-x}Dy_xMnO_3$.

2. Experimental procedure

$Tb_{1-x}Dy_xMnO_3$ with $x=0.0$, 0.3, 0.5, 0.6, and 0.8, were prepared by the conventional solid-state reaction method. Appropriate amounts of high-purity Tb_4O_7, Dy_2O_3 and Mn_3O_4 powders were weighed according to the nominal formula, mixed and ground carefully, then pressed into large discs of 30 mm diameter under 250 MPa and presintered at 1000 °C for 10 h. After that, the discs were crushed, ground again and pressed into pellets with a diameter of 15 mm and a thickness of 2 mm at 300 MPa, and finally sintered for 10 h at 1280 °C. X-ray diffraction (XRD), using a D-Max Rigaku system with the Cu$K\alpha$ radiation and a graphite monochromator, was employed to investigate the structure of the samples at room temperature. As a function of T and H, the magnetization (M) was measured on a Quantum Design MPMS SQUID magnetometer (Quantum Design MPMS-XL, USA).

3. Experimental results and discussion

The structural characterization of sintered $Tb_{1-x}Dy_xMnO_3$ samples detected by powder X-ray diffraction is shown in Fig. 1(a),

* Corresponding author. Tel.: +86 25 83587428; fax: +86 25 83587443.
E-mail addresses: meihua_xu@126.com, xumeihua@njut.edu.cn (M.H. Xu).

0304-8853/$ - see front matter © 2013 Elsevier B.V. All rights reserved.
http://dx.doi.org/10.1016/j.jmmm.2013.03.022

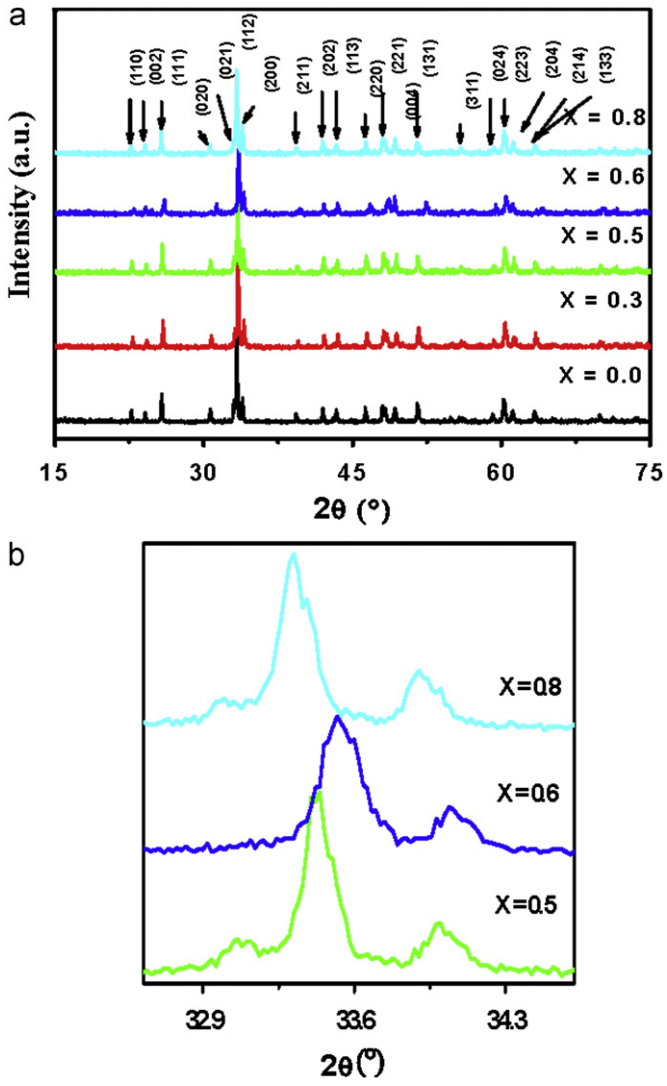

Fig. 1. (a) X-ray diffraction patterns for $Tb_{1-x}Dy_xMnO_3$ samples at room temperature. (b) The enlarged view at about $2\theta=33.30^\circ$ region are displayed.

which can be well indexed by an orthorhombic structure with a space group Pbnm (No: 62)(JCPDS Card File No. 72-0379) indicating high purity of the samples. Because Dy^{3+} ionic radius (0.091 nm) is almost equal to Tb^{3+} ionic radius (0.092 nm), the lattice constant of $Tb_{1-x}Dy_xMnO_3$ is invariable and the diffraction peak shows an immeasurable shift with increasing Dy content. However, we can find a slight difference of the peaks near 33.30°. There are two peaks for the structure with $x=0.6$ (Fig. 1(b)) while there are three peaks for the structures with $x=0.0$, 0.3, 0.5, and 0.8 near 33.30°. Moreover a slight shift to higher 2θ for $x=0.6$ sample is observed distinctly in Fig. 1(b). Arima et al. reported the transformation of the Mn-spin alignment from sinusoidal (collinear) AFM into a transverse-spiral structure by a neutron diffraction study for $x=0.59$ (close to 0.6) of $Tb_{1-x}Dy_xMnO_3$ [23]. It is well known that the spin state of magnetic ion can lead to the change of magnetic property of manganite and strong coupling between the magnetic property and crystal lattice [24,25]. Hereby we surmise that there may be a slight structure and/or symmetry change coming from magnetic transition for $Tb_{0.4}Dy_{0.6}MnO_3$. This issue remains to be further studied.

Shown in Fig. 2 are the curves of magnetization (M) versus temperature collected on $Tb_{0.4}Dy_{0.6}MnO_3$ sample in zero field cooled (ZFC) and field cooled (FC) processes (applied field, 10 Oe). The ZFC curve shows a peak around 37 K which is

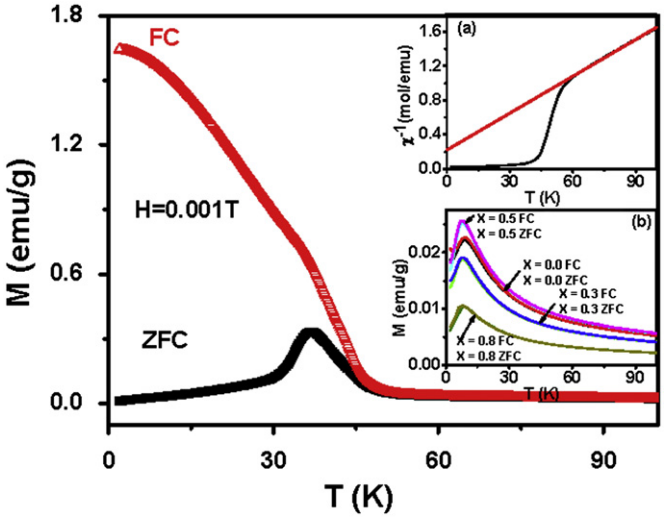

Fig. 2. Temperature dependence of ZFC and FC magnetizations measured at a field (H)=10 Oe for $Tb_{0.4}Dy_{0.6}MnO_3$. Inset: (a) inverse magnetic susceptibility with temperature measured at $H=10$ Oe. (b) Temperature dependence of ZFC and FC magnetizations measured at a field (H)=10 Oe for $Tb_{1-x}Dy_xMnO_3$ (x=0.0, 0.3, 0.5, and 0.8).

suggested to be the Néel temperature (T_N). The ZFC magnetization shows a typical antiferromagnetic (AFM) characteristic. This is analogous to that observed in similar isovalent substituted compounds exhibiting A-type AFM ordering such as $Eu_{1-x}Y_xMnO_3$ [18], $La_{1-x}Eu_xMnO_3$ [20], $La_{1-x}Gd_xMnO_3$ [21], $Tb_{1-x}Dy_xMnO_3$ [23] and $Eu_{1-x}Sm_xMnO_3$ [26]. The ZFC and FC $M(T)$ curves bifurcate at $T_B=50$ K, which is higher than T_N. Chen et al. ascribed such behavior in $La_{1-x}Eu_xMnO_3$ to a two-dimensional (2D) ferromagnet (FM) fluctuation arising from the 2D FM ordering of Mn spins in the *ab* plane [20]. The FC and ZFC magnetizations have the same value above 50 K. Below 50 K, FC magnetization ascends rapidly with decreasing temperature to about 10 K and then increases slowly. Our result may hint the presence of FM phase or spin glass like (SGL) phase in AFM compound $Tb_{0.4}Dy_{0.6}MnO_3$ at low temperature.

The inset of Fig. 2(a) shows the inverse susceptibility (χ^{-1}) for $Tb_{0.4}Dy_{0.6}MnO_3$. We have analyzed the data using the following equation:

$$\chi(T)=\frac{C}{T-\theta_{CW}}$$

where C is the Curie constant and θ_{CW} is the Curie–Weiss temperature. We obtained $C=64.21$ K emu mol^{-1} and $\theta_{CW}=-15.48$ K. For higher temperature, the susceptibility (χ) follows the Curie–Weiss (CW) law as clearly revealed by the linear inverse susceptibility with an effective paramagnetic moment $\mu_{eff}=22.62\mu_B$, which is attributed mainly to paramagnetic Tb^{3+}, $Dy^{3+}$and Mn^{3+} ions. The curves of M versus temperature collected on $Tb_{1-x}Dy_xMnO_3$ (x=0.0, 0.3, 0.5, and 0.8) samples in ZFC and FC processes (applied field, 10 Oe) are shown in the inset of Fig. 2(b). Both ZFC and FC magnetizations show typical characteristic of an AFM for x=0.0, 0.3, 0.5, and 0.8.

In order to explore the magnetic property at low temperature, we have measured the magnetic hysteresis (M–H loop) for $Tb_{1-x}Dy_xMnO_3$ at 5 K. The M–H loop for $Tb_{0.4}Dy_{0.6}MnO_3$ is also different from that for $Tb_{1-x}Dy_xMnO_3$ (x=0.0, 0.3, 0.5, and 0.8). The typical results are shown in Fig. 3 and its inset for $Tb_{0.5}Dy_{0.5}MnO_3$. The shape of M–H loop indicates that there is superposition of FM loop and AFM loop. M is still unsaturated in a magnetic field as strong as 5 T. Considerably high coercivity H_C (~6 kOe) is suggested due to the coexisting magnetic phases as well as the magnetocrystalline anisotropy. The shape of M–H loop